

# We are IntechOpen, the world's leading publisher of Open Access books Built by scientists, for scientists

**4,800**

Open access books available

**122,000**

International authors and editors

**135M**

Downloads

Our authors are among the

**154**

Countries delivered to

**TOP 1%**

most cited scientists

**12.2%**

Contributors from top 500 universities



**WEB OF SCIENCE™**

Selection of our books indexed in the Book Citation Index  
in Web of Science™ Core Collection (BKCI)

Interested in publishing with us?  
Contact [book.department@intechopen.com](mailto:book.department@intechopen.com)

Numbers displayed above are based on latest data collected.

For more information visit [www.intechopen.com](http://www.intechopen.com)



## Mechanism of Pit Growth in Homogeneous Aluminum Alloys

G. Knörnschild

*Federal University of Rio Grande do Sul  
Brazil*

### 1. Introduction

Pitting corrosion is a process, which takes place on passive metals and alloys. A characteristic of this type of corrosion is that passivity breaks down at isolated points at the surface and the growth of pits is observed due to locally high rates of metal dissolution. In electrochemical experiments, the growth of pits leads to a rapid rise of the overall current density once a characteristic threshold potential, the pitting potential  $E(\text{pit})$  is surpassed. Since the measured current density is composed of the passive current density at the passive surface area and the current density of fast metal dissolution at the pitted area conventional electrochemical tests are not useful for studying metal dissolution inside pits. Some authors tried to overcome this difficulty by working with small wire electrodes. The idea behind was to achieve an electrode state where the whole surface represents a pit and the measured current density becomes, therefore, identical to the real current density inside a pit. However, highly concentrated electrolytes and high potentials must usually be applied to achieve this electrode state [1-3]. Formation of salt films and mass transport control was usually observed under these conditions, which more likely represent the conditions of electropolishing rather than that of a metal suffering pitting corrosion at the corrosion potential.

Other authors determined the current density during the initial stage of pit growth from the microscopic measurement of the dimensions of pits formed in short time experiments [4]. By measuring the time for perforation by pitting of thin metal foils Hunkeler [5] and Cheung [6] obtained average rates of pit growth, i.e., average current densities normal to the foil surface. Average rates of localized corrosion at grain boundaries of aged AlCu alloys have been determined by metallographic measurements of penetration depth and penetration time [7]. By the same method early stages of pit propagation were studied in 7075-T3 alloy [8]. Few studies have been made to measure in-situ metal dissolution inside pits. Edeleanu [9] examined the pit propagation in thin aluminum foils, glued to a glass foil which could be observed from the back side by a microscope. In this way pit propagation along the glass foil could be observed in situ. The technique was applied again for an intensive study of pit growth in pure aluminum by Baumgärtner [10-12], and for the study of homogeneous aluminum alloys by Knörnschild and Kaesche [13,14]. Later, Frankel [15] used a similar technique to study pit growth in thin aluminum films deposited by PVD.

## 2. Experimental techniques

Pure aluminum as well as homogeneous Al-4wt.%Cu and Al-3wt.%Zn alloys were studied in NaCl and AlCl<sub>3</sub>-solutions of varying concentrations, using a conventional three-electrode-arrangement. Tests were performed either in potentiostatic, potentiodynamic or galvanostatic mode. Samples were homogenized by annealing for one hour at 480°C (Al), 530°C (AlCu) and 400°C (AlZn), respectively. After annealing the samples were quenched in cold water. The cold water quench of AlCu was interrupted for five seconds in boiling water in order to prevent accelerated clustering of copper due to quenching stresses.

The experimental arrangement for the microscopic observation of pit growth is shown in Fig.1. The thin samples were glued to a glass foil which formed the bottom of the electrochemical cell. The lower side of the sample could be observed by a microscope and filmed with a coupled camera. The samples were polarized potentiostatically or galvanostatically in chloride solution. In samples with (100)-orientation metal dissolution during pitting occurs perpendicular to the glass foil surface. Once a pit has grown enough to reach the glass foil the current density of metal dissolution can be determined by image analysis from the shift of the tunnel front.

Tunnels in AlZn alloy were further studied by an oxide replica technique; i.e., the pitted samples were anodized during 60s at 70V in NH<sub>4</sub>H<sub>2</sub>PO<sub>4</sub>-electrolyte and the metal was chemically dissolved in a methanolic Br<sub>2</sub> solution, leaving only the anodic oxide film.

The current densities of hydrogen evolution during pitting were determined volumetrically by the collection of the evolved H<sub>2</sub> gas.

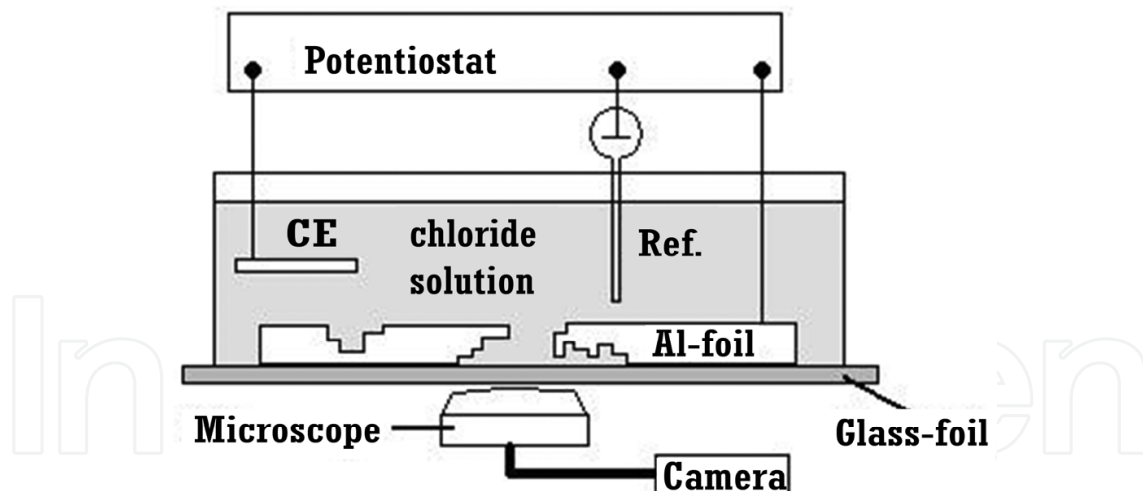


Fig. 1. Experimental arrangement for microscopic observation of pit growth.

## 3. Results

### 3.1 Morphology of pitting attack

#### 3.1.1 Al and AlCu-alloy

Pure aluminum and the homogeneous aluminum alloys have a pronounced pitting potential  $E(\text{pit})$  in 1M NaCl solution. Stationary potentiostatic or galvanostatic measurements show

that the electrodes become nearly unpolarizable at this threshold potential (Fig.2). Metal dissolution during pitting in aluminum and in homogeneous aluminum alloys at or above this threshold potential leads to the formation of crystallographic pits. In the AlCu alloy, pits grown in chloride solution have walls, which consist of (100)-planes (Fig.3). In principle, the morphology is identical with that observed in pure aluminum. However, while pure aluminum pits shows sharp (100)-planes (Fig.4), rounded walls are more frequently found in the AlCu alloy (Fig.3). Transmission electron microscopy of pitted samples revealed that these rounded walls consist of fine crystallographic (100)-steps (Fig.5). It was also observed that more corrosion products, frequently containing Cu, are found at the surface of pits in AlCu than in pure Al.

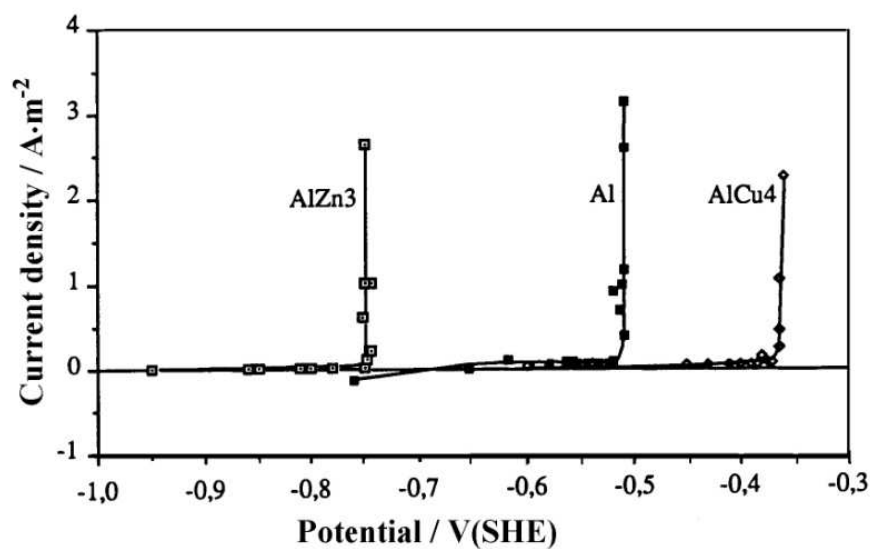


Fig. 2. Stationary current density - potential curve of Al, homogeneous Al-4wt.%Cu and homogeneous Al-3wt.%Zn in deaerated 1M NaCl solution.

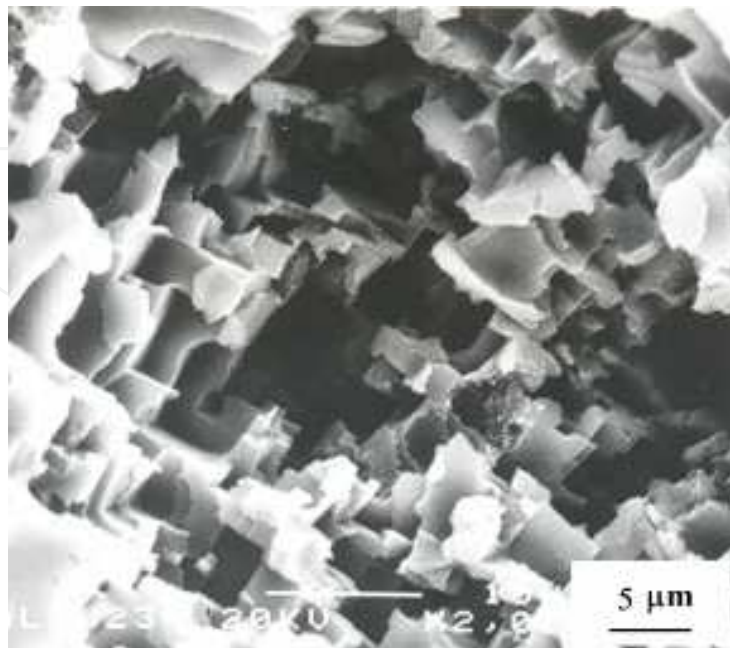


Fig. 3a. Morphology of pits in the the AlCu alloy in 1M NaCl.

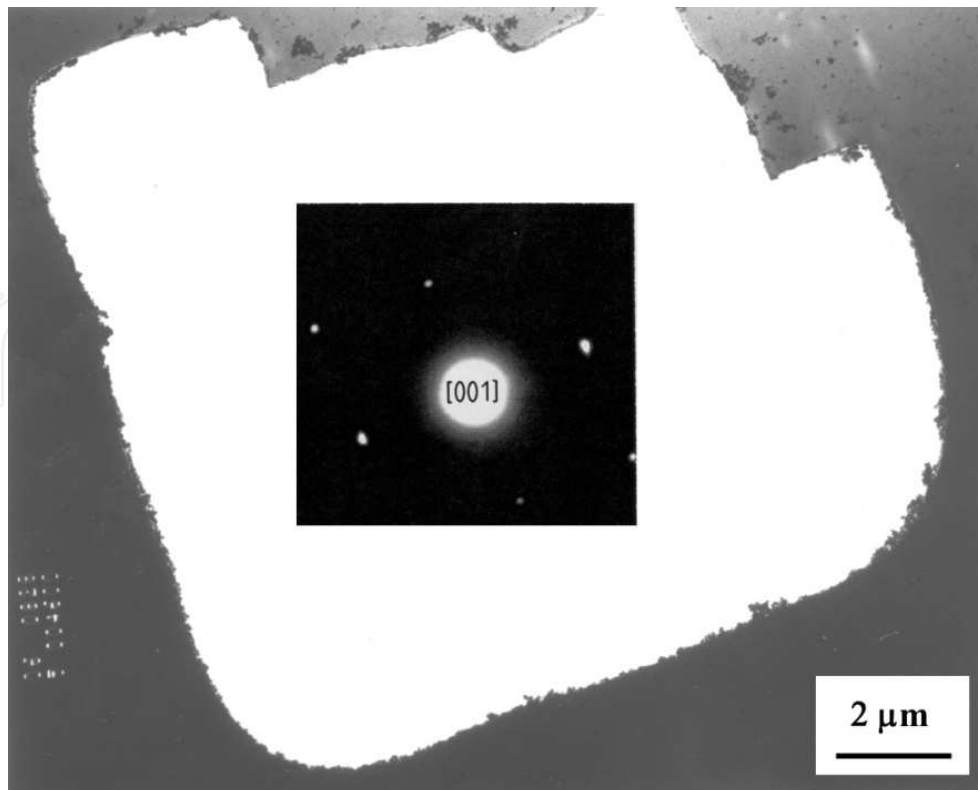


Fig. 3b. Transmission electron micrograph of pit in the AlCu-alloy with corresponding electron diffraction pattern showing (100) pit walls.

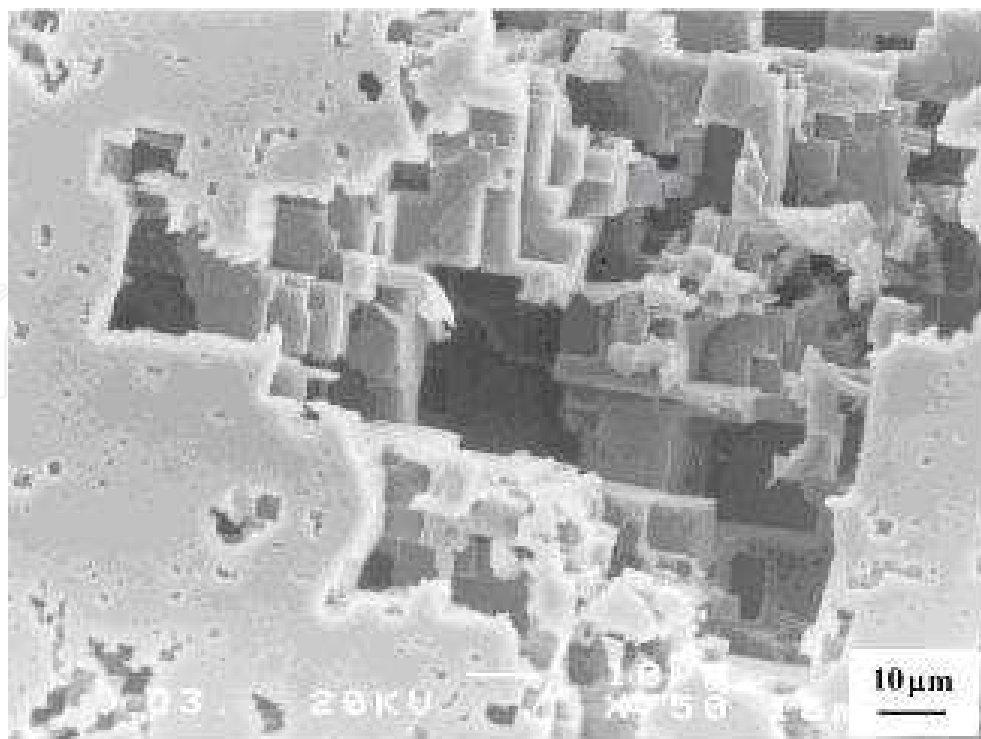


Fig. 4. Morphology of pits in pure Al in 1M NaCl.

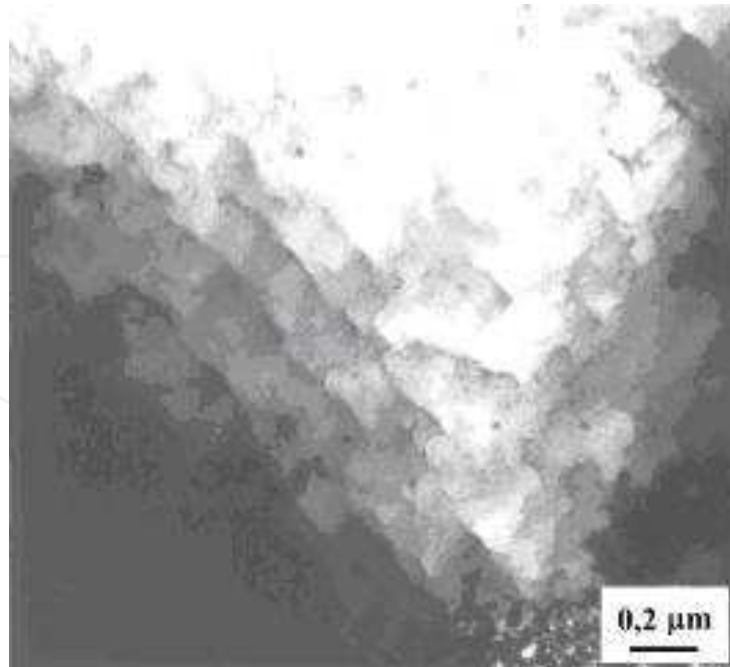


Fig. 5. Transmission electron micrograph of AlCu-alloy showing crystallographic fine structure of rounded pit walls.

### 3.1.2 AlZn-alloy

In the homogeneous AlZn alloy tunnels with rounded cross section grow in crystallographic directions (Fig.6). Growth directions have been confirmed as  $\langle 100 \rangle$  directions by electron diffraction of pitted TEM samples. Tunnel diameters are up to  $0,5\mu\text{m}$ . The morphology is very similar to tunnels which grow in pure aluminum in hot hydrochloric acid. These conditions are widely used for the etching of capacitor foils [16]. The tunnels in capacitor foils, however, have a quadratic cross section, i.e., the tunnel side walls are crystallographic.

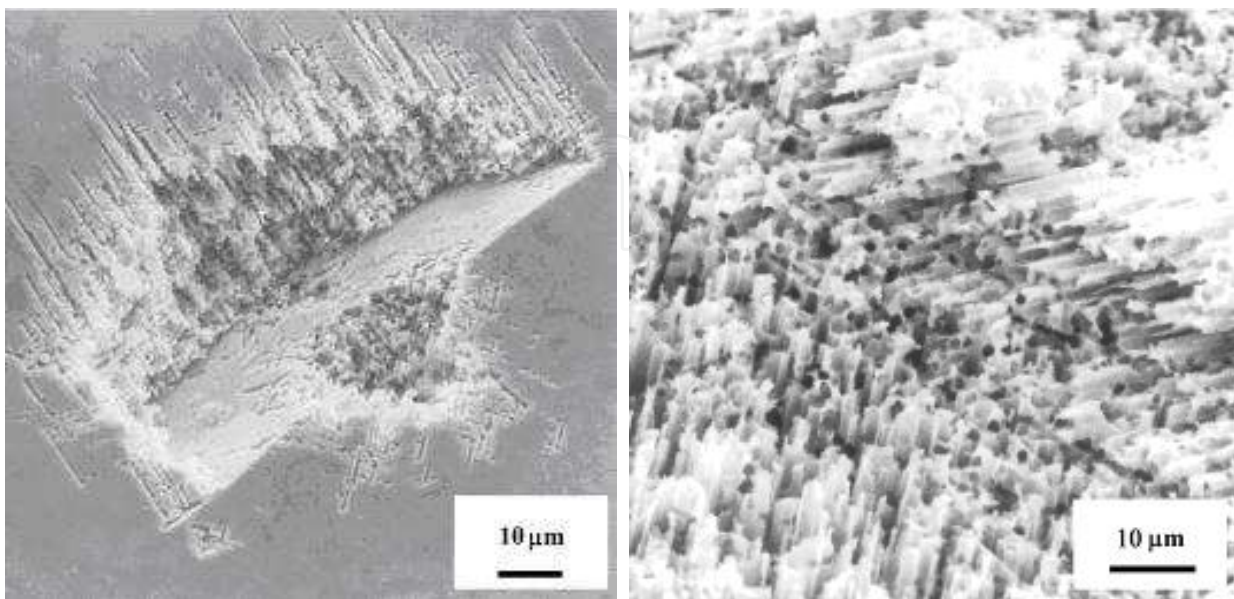


Fig. 6a,b. Pitting attack in AlZn alloy in 1M NaCl, showing accumulation of tunnels.

In the case of tunnels in AlZn only the growth direction is crystallographic, while the side walls do not show any crystallographic aspects, as confirmed by TEM examinations (Fig.7). When tunnels in AlZn are produced in acid chloride solution they show crystallographic cross sections like capacitor foils, even when produced at room temperature (Fig.8). A drawback for the industrial use of the AlZn tunnels is that they show a strong tendency to clustering (Fig.6 and 9) instead of a uniform tunnel distribution. A great number of parallel tunnels usually starts to grow from the same point of attack (Fig.9).

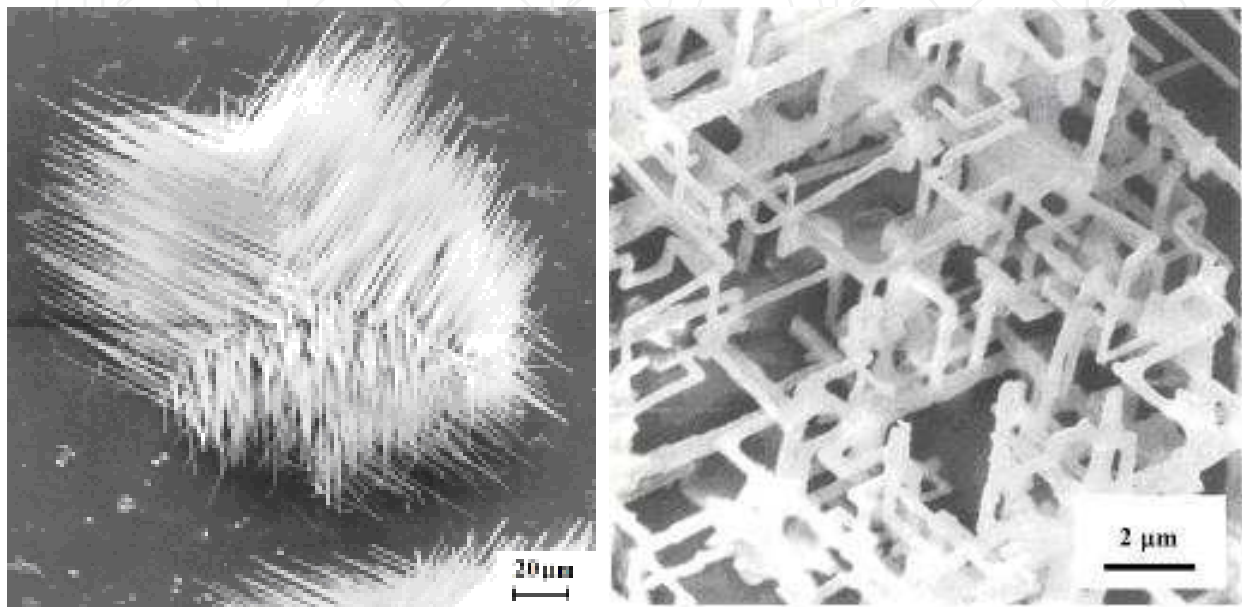


Fig. 6c,d. Tunnels in AlZn alloy in 1M NaCl, revealed by oxide replica technique.

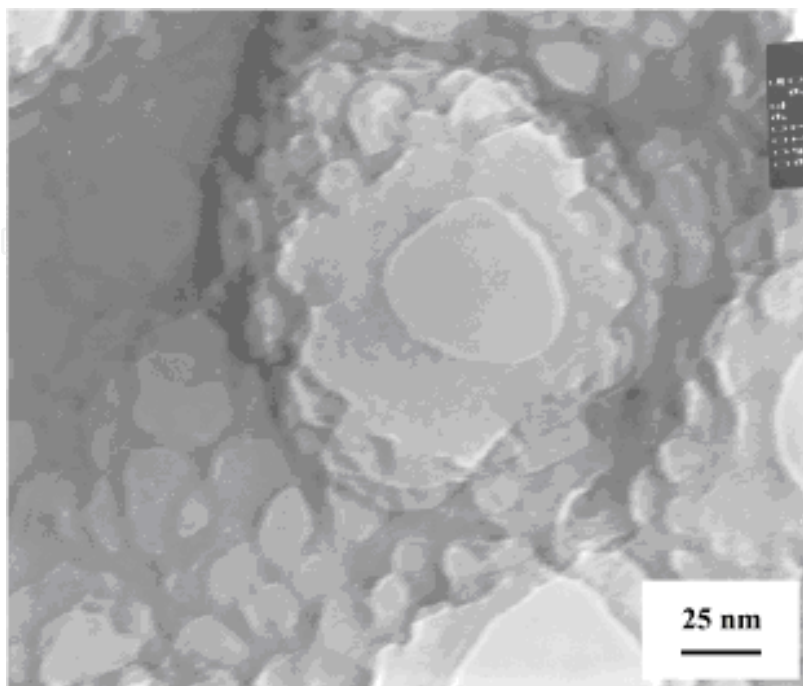


Fig. 7. Transmission electron micrograph of tunnel walls in AlZn-alloy.

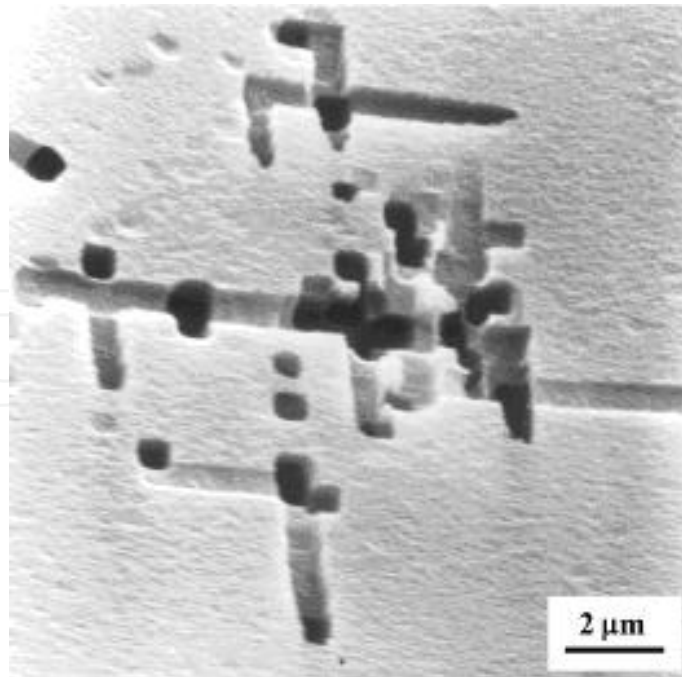


Fig. 8. AlZn: Tunnels with quadratic cross section grown in solution of NaCl, pH1,5.

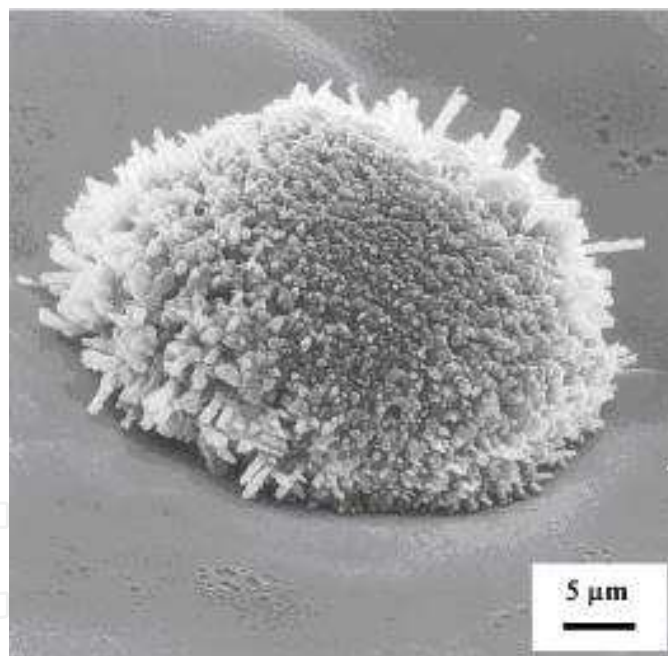


Fig. 9. AlZn-alloy: Early stages of tunnel growth in 1M NaCl solution.

### 3.2 Pit propagation studied by in-situ microscopic observation

#### 3.2.1 AlCu-alloy

The growth of pits occurs by subsequent dissolution of crystallographic steps at (100)-planes. By periodic restriction of the area of the dissolving planes a tunnel-like morphology is formed, in the example shown in Fig.10 this tunnel propagates approximately in  $\langle 110 \rangle$ -direction.



The life time of localized dissolution events, such as that shown in Fig.10 is limited, even at or above the pitting potential. Repassivation may occur after some seconds or localized dissolution may last up to about one minute. At higher applied potentials life time tends to be longer. While one tunnel repassivates, other tunnels begin to propagate. This means that macroscopic pits are formed by a great number of localized, short-lived dissolution events, occurring simultaneously and subsequently. At any time, only a small part of the inner surface of a macroscopic pit is actively dissolving. The formation of macroscopic pits probably happens due to the fact that in front of recently repassivated surfaces the electrolyte is enriched in aluminum and chloride ions. This environment with low pH and high concentration of passivity destroying ions makes the nucleation of new tunnels more probable in comparison to nucleation at the passive surface outside the pit.

From the shift of the crystallographic planes the average current density during pit growth was calculated by Faraday's law. The current densities, obtained from testes in diluted NaCl solutions vary between  $3\text{A}/\text{cm}^2$  and  $10\text{A}/\text{cm}^2$  (Fig.11). In the case of pure aluminum, the same average current densities were obtained in diluted NaCl solution [10-12], however, up to  $30\text{A}/\text{cm}^2$  were measured during short time intervals, proving that the dissolution of the crystallographic fronts indeed is a discontinuous process. In the case of the homogeneous AlCu alloy signs of discontinuous propagations were also found. However, discontinuities seem to be at a finer scale and are therefore close to the spatial resolution of the microscope.

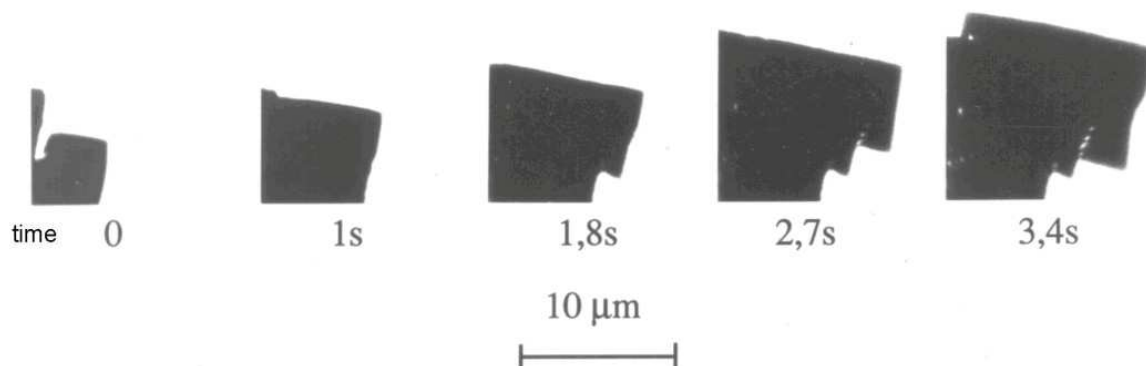


Fig. 10. Microscopic in-situ observation of tunnel growth in AlCu-alloy. Electrolyte: 1M NaCl.

Average current densities remain almost constant during tunnel propagation, as can be seen in Fig.11. In no case the current density depended on the pit depth or tunnel length. It was also confirmed that chloride concentration (except saturated  $\text{AlCl}_3 \cdot 6\text{H}_2\text{O}$  solution, as described below), as well as applied potential above  $E(\text{pit})$  and applied current density in galvanostatic tests have no influence on the measured average current density of actively dissolving tunnel fronts.

Dissolving tunnel fronts stopped immediately, i.e., within tenths of a second, when the potential was switched below the pitting potential  $E(\text{pit})$  indicated in the stationary current density-potential-curve. The behavior of growing tunnels during potential switch experiments to  $E < E(\text{pit})$  has been intensively studied for pure aluminum in NaCl solution by Baumgärtner [10-12]. It was found that the time to repassivation was shorter the lower

the potential  $E < E(\text{pit})$  to which the potential was switched. The tests fulfilled with the homogeneous AlCu alloy indicated that the behavior of the alloy is qualitatively the same.

The only influence on the current density of growing tunnel fronts was found in highly concentrated or saturated  $\text{AlCl}_3 \cdot 6\text{H}_2\text{O}$  solution. In this case the shift of broad dissolution fronts instead of rather large (100) planes is observed. Ex-situ electron microscopy revealed that the dissolution front in concentrated or saturated  $\text{AlCl}_3 \cdot 6\text{H}_2\text{O}$  solution has also a fine structure of (100) steps. The average current density of aluminum dissolution under these conditions was in the order of  $0,3\text{A}/\text{cm}^2$ , which means one order of magnitude below that in diluted chloride solutions. Here, again, pure aluminum and homogeneous AlCu alloy showed very similar results.

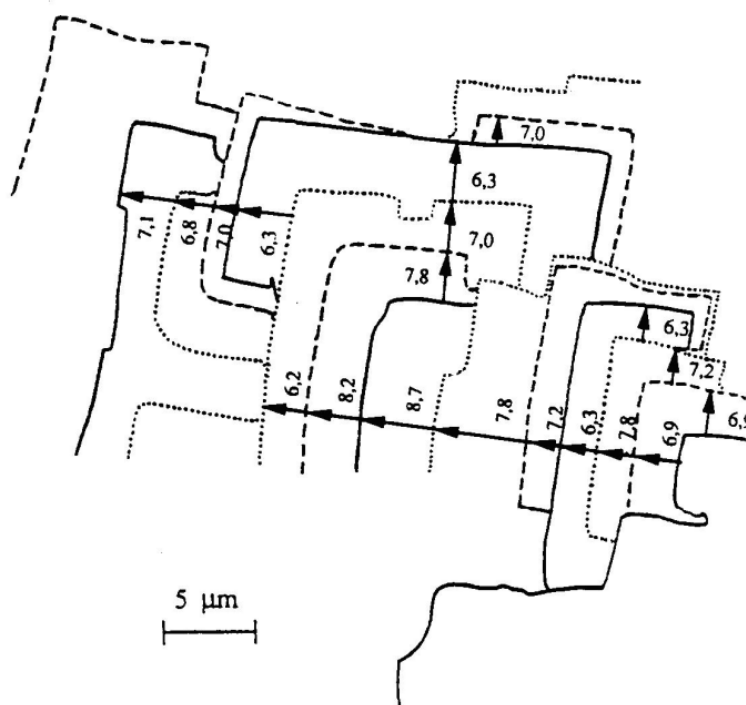


Fig. 11. Propagation of tunnel front in AlCu alloy, obtained from in-situ observations. Electrolyte: 1M NaCl. Time interval between two lines: one second; numbers indicate current density in  $\text{A}/\text{cm}^2$ .

### 3.2.2 AlZn-alloy

In the homogeneous AlZn alloy one-dimensional growth of tunnels with cylindrical cross section of some tenths of  $\mu\text{m}$  in crystallographic directions is observed (Fig.6). The tunnel diameter remains constant over the tunnel length, which means that dissolution of the tunnel walls is negligible in comparison to the dissolution at the tunnel tip.

As in the case of pure aluminum and the AlCu alloy the rate of metal dissolution, in this case the propagation of the tunnel tip, did not depend on tunnel length, as can be seen in Fig.12. Current densities at the tunnel tip, obtained from this and from other experiments in diluted NaCl solution were about  $5\text{A}/\text{cm}^2$ . The in-situ microscopic technique is not very appropriate for the observation of the one dimensional tunnels in the AlZn alloy, since it

needs a great number of experiments to find tunnels which propagate exactly in the plane of the glass foil. Therefore additional short time experiments were made with conventional samples. The average current density of tunnel propagation was calculated from the tunnel length, measured by the oxide replica technique and the time of tunnel growth (being supposedly equal to the duration of the experiment). Average current densities between 2 and 7 A/cm<sup>2</sup> were obtained in this way. This means, that the values are in the same order of magnitude as in the case of aluminum and of the AlCu alloy. The tunnel life in AlZn alloys is also limited. The maximum tunnel length registered in all the tests performed with the AlZn alloy was about 100 μm (Fig.6a,c).

Again, as in the case of aluminum and of the AlCu alloy, chloride concentration, applied potential or applied current density in galvanostatic tests have no influence on the current density. The only condition, where different results are obtained, is again saturated AlCl<sub>3</sub>·6H<sub>2</sub>O solution: In the case of the AlZn alloy the tunnel length in saturated AlCl<sub>3</sub>·6H<sub>2</sub>O solution is shorter than in diluted chloride solutions, i.e. tunnel life times are shorter. Because of the very short life time of these tunnels the current densities could not be determined under these conditions.

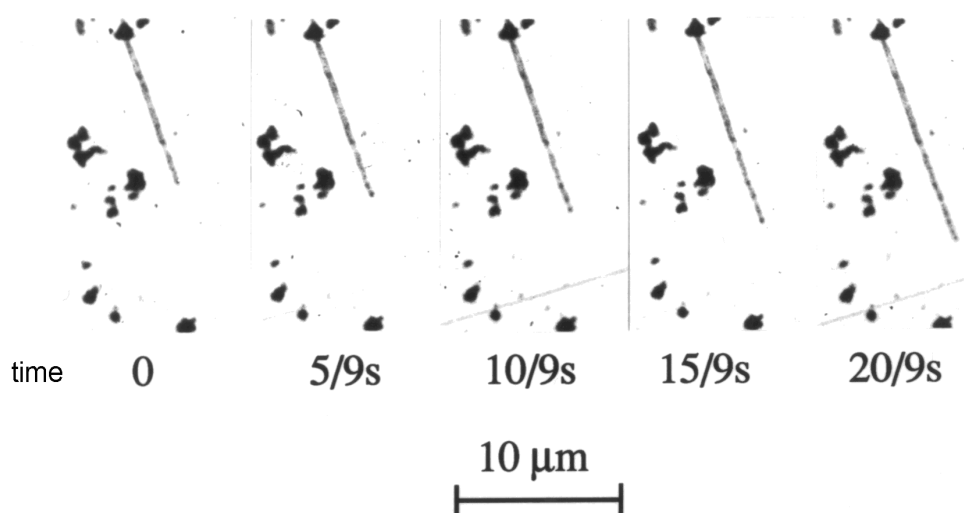


Fig. 12. Microscopic in-situ observation of tunnel growth in AlZn. Electrolyte: 1M NaCl.

### 3.3 Hydrogen evolution as a partial reaction during pitting

Nucleation of H<sub>2</sub> bubbles can be observed during pitting in pure aluminum and in the AlCu alloy. By microscopic in situ observations it becomes clear that hydrogen evolution is spatially correlated with sites of fast active metal dissolution inside pits, however, this doesn't mean that bubble formation occurs directly at the active pit surface. In the fine tunnels in AlZn bubble nucleation cannot take place during tunnel growth, since bubble formation would block completely the potential control of the tunnel front. This is also confirmed by microscopic observations. During tunnel growth formation of bubbles was not observed inside the tunnels. However, sometimes bubbles formed inside a tunnel after its repassivation. From these observations it becomes clear that mass transport inside growing AlZn tunnels is not accelerated by hydrogen bubbles and that blockage of potential control at the tunnel tip by bubbles is not the reason for repassivation.

Volumetric measurements of hydrogen evolution accompanying pitting corrosion showed a characteristic value of  $i(H)/i(Al)$ , without considerable dependence of the chloride concentration (Fig.13). No appreciable change was observed when tests were performed in diluted iodide solutions. Also, the differences between Al, AlCu and AlZn were small. In all the performed tests the ratio  $i(H)/i(Al)$  remained in the interval between 0,09 and 0,17. The variation of the pitting potential  $E(pit)$  in these tests was almost 800mV (Fig.13). Consequently,  $i(H)/i(Al)$  does not depend on the electrode potential.

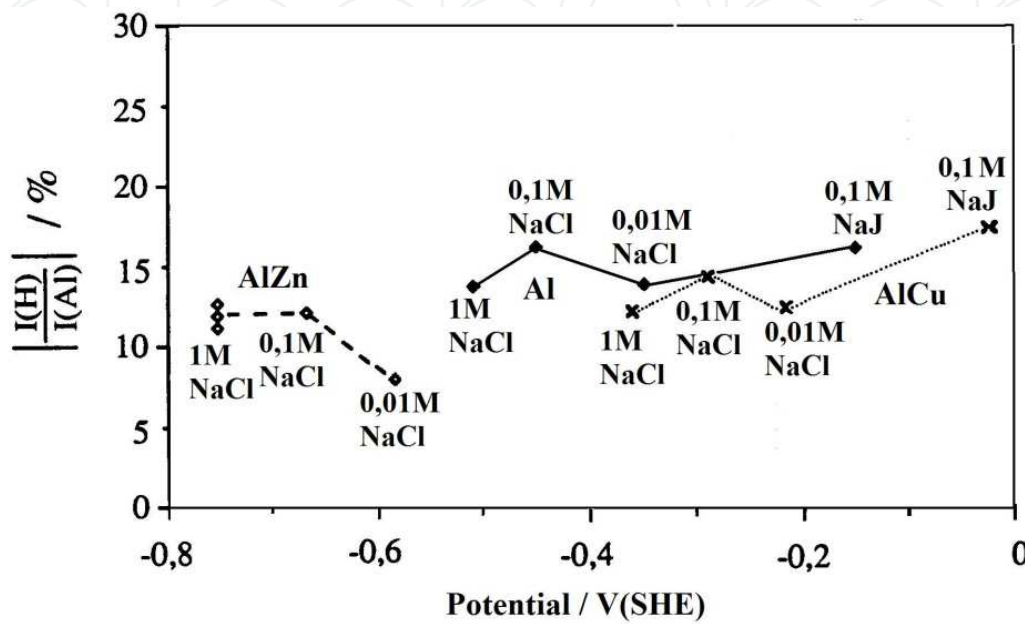


Fig. 13. Relation of current densities of hydrogen reduction  $i(H)$  to Al-dissolution during pitting  $i(Al)$ . Volumetric measurements with Al, AlCu and AlZn in chloride and iodide solutions.

#### 4. Discussion and conclusions

The present work has shown that macroscopic pitting is the result of the growth of isolated tunnels. Each one of these tunnels has a limited lifetime. At any time only a small area is active within a macroscopic pit. This behavior explains why current densities measured in-situ at active tunnel fronts are much higher than current densities obtained from the penetration time by pitting of thick specimens. Even in penetration experiments with thin foils as those performed by [5,6] penetration times may be longer than single short-lived active dissolution events which can be observed by microscopic in-situ experiments. In this case, current densities, calculated from penetration times, are averaged values which contain periods of rapid local dissolution and times of standstill. Therefore, one has to be careful with conclusions about dissolution kinetics, which were drawn, for example, from the potential dependence or and the thickness dependence of the results.

In situ pit growth experiments have shown that the current density of Al dissolution at actively dissolving pit fronts is practically independent of the alloy composition for pure Al, homogeneous AlZn and AlCu alloy, as well as independent of the externally applied electrode potential. This has been confirmed in tests with the different alloys and with

different chloride concentrations, in which the potential variation was more than 0.5V. Current density of metal dissolution, when measured in time intervals of some tenths of a second always remained in the range of 3 - 10A/cm<sup>2</sup>. The independence of metal dissolution rate from applied electrode potential could be interpreted as mass transport control. However, from the fact that the dissolution rate of active pit fronts depends neither on the tunnel length nor on the concentration of Al<sup>3+</sup> and Cl<sup>-</sup> in the bulk electrolyte transport control of Al dissolution during pitting can be ruled out. Volumetric tests showed that the rate of hydrogen evolution accompanying pitting of Al, AlCu and AlZn is related to the rate of Al dissolution. I.e., the relation of  $i_H/i_{Al}$  varies between 0.09 and 0.17, independent of externally applied current or potential, chloride or iodide concentration. This was found for the current densities related to the geometrical surface of the samples, but certainly this also holds for the true local current densities  $I_H$  and  $I_{Al}$  inside the pits. The volumetric tests were performed within a potential range of about 0.8V, so the relation of  $I_H/I_{Al}$  can be considered independent of the applied potential.

The results about Al dissolution and hydrogen evolution show that the two reactions are coupled. They do not represent independent partial reactions. From these results it becomes obvious that at the active pit front always the same conditions are maintained, characterized by a typical current density of Al dissolution of 3-10A/cm<sup>2</sup>, and a current density of hydrogen evolution which is between 9 and 17% of the anodic current density. This holds independent of the set of external parameters: applied current density, applied potential, kind and concentration of halide ion and Al<sup>3+</sup> in the bulk electrolyte; nearly saturated AlCl<sub>3</sub>·6H<sub>2</sub>O solution being the only exception.

The fact that Al dissolution in highly concentrated AlCl<sub>3</sub>·6H<sub>2</sub>O solutions with a pH ≈ 0 is considerably slower than dissolution in neutral bulk NaCl solution shows that acidification alone is not the critical factor which allows the special kind of high rate metal dissolution occurring during pitting of Al. It rather points to the existence of a metastable surface film which permits metal dissolution into an electrolyte which is normally not saturated with respect to the film forming ions. In principle this is the same situation which is found in most cases of passivity. The passive film is usually thermodynamically unstable, since the electrolyte is not saturated with respect to the passive film. In practice, most passive films are protective because of the slow dissolution kinetics not because of its thermodynamic stability. In the case of pitting the only difference is the high rate of film formation and dissolution.

Although further information about the exact nature of the film is not available, it is clear that the active Al surface must be covered by chloride or some oxychloride species, since otherwise Al would passivate in the aqueous environment. The film permits the fast passage of Al ions and can consequently be considered an AlCl<sub>3</sub>-film. Kaesche [14] describes this salt film as AlCl<sub>z</sub>·xH<sub>2</sub>O, which means that its exact stoichiometry and its degree of hydration are not known. Beck [1] concluded from experiments with wire electrodes that an anhydrous film exists at the metal surface and that this film is hydrated from the electrolyte side. Beck found that at sufficiently high potentials and in highly concentrated AlCl<sub>3</sub> electrolyte salt film dissolution becomes mass transport controlled. Under these conditions the film thickens and water diffusion into the film to the metal-film interface determines the rate of hydrogen reduction. With growing potential and thus growing film thickness the ratio  $I_H/I_{Al}$  diminishes. The same observation Beck made for mass transport controlled dissolution of Mg [3].

This model means that hydrogen is reduced at the metal-film interface and that reduced hydrogen must diffuse back through the film to the electrolyte, where bubble formation occurs. It should be mentioned that an alternative, well known model for hydrogen evolution during pitting exists: Dissolution of Al as  $\text{Al}^{2+}$  or  $\text{Al}^+$  and further oxidation of these ions by  $\text{H}^+$  in a homogeneous reaction. The fact that in the present work a characteristic current density of Al dissolution and a characteristic ratio of  $I_{\text{H}}/I_{\text{Al}}$  were found in all cases might show that these conditions are indispensable for the kind of metal dissolution during pitting of Al.

Parting from Beck's model that water is transported through the salt film, a constant ratio of  $I(\text{H})/I(\text{Al})$  might indicate, that the high dissolution current is necessary to hold the  $\text{O}^{2-}/\text{Cl}^-$  ratio ( $\text{O}^{2-}$ -formation by  $\text{H}_2\text{O} + 2\text{e}^- \rightarrow 2\text{H} + \text{O}^{2-}$ ) at the metal surface below a critical value. Slower metal dissolution makes the  $\text{O}^{2-}$  coverage of the metal surface rise and causes repassivation. Obviously, this condition is affected when dissolution of Al becomes controlled by diffusion. Simple estimations for the  $\text{Al}^{3+}$  transport show that it is difficult to maintain current densities of some  $\text{A}/\text{cm}^2$ , when the diffusion layer reaches the order of 100  $\mu\text{m}$ . The assumption of repassivation by beginning transport control is sustained by various experimental observations: Tunnel length in the AlZn alloy is limited to about 100  $\mu\text{m}$ . Studies of tunnel growth in aluminum at about 80°C in HCl, from Alkire [16], also showed tunnels, whose length do not surpass 100  $\mu\text{m}$ . In another work, it was shown that the tunnel length in aluminum at 70°C diminishes with growing  $\text{AlCl}_3$  concentration in the electrolyte [17]. In the present work tunnels in the AlZn alloy reached only a length of a few  $\mu\text{m}$  in saturated  $\text{AlCl}_3 \cdot 6\text{H}_2\text{O}$  solution.

Al and AlCu in saturated  $\text{AlCl}_3 \cdot 6\text{H}_2\text{O}$  solution can maintain the necessary high current density for tunnel growth only during very short time intervals, due to the slow transport between the surface with some supersaturated  $\text{AlCl}_3$  film and the  $\text{AlCl}_3 \cdot 6\text{H}_2\text{O}$  saturated electrolyte. Pit growth stops due to beginning transport control but restarts moments later when the concentration has declined. As a result of the discontinuous propagation the average current density of Al dissolution is lower.

Hebert and Alkire [18] also considered diffusion as the decisive factor for repassivation. According to these authors the growth of one-dimensional tunnels stops when the diffusion layer extends over the whole tunnel length and the tunnel tip becomes saturated with  $\text{AlCl}_3 \cdot 6\text{H}_2\text{O}$ .

Kaesche [14] suggested that the sum of diffusion potential and ohmic potential drop rises during tunnel growth and repassivation occurs when the potential at the tunnel bottom falls below some critical value. From the thermodynamic point of view the critical value is the equilibrium potential of the film forming reaction.

Potential switch experiments showed that the external potential where repassivation of growing pits occur is identical with the potential  $E(\text{pit})$  obtained from the steep rise of the stationary current density – potential curve.

Separate pitting and repassivation potentials are found especially in works about metastable alloys [19]. These are interesting because alloys supersaturated with alloying elements like Mo, W, Ta [20-22] have much higher pitting potentials than those that can be achieved by conventional alloys like Al-Cu. Due to the fabrication process, PVD techniques or rapid

solidifying these alloys are only available as very thin films or melt spun ribbons. Recent progress in producing supersaturated bulk materials is so far restricted to alloying systems based on Zr, Fe, Ni and Cu [23]. The problem with the reported pitting potentials is that, due to the thin format of the samples, measurements are generally made non-stationary by potentiodynamic tests.

The question of repassivation was sometimes also discussed because the reverse scan of potentiodynamic tests reveals that pitted samples show considerably higher current densities below  $E(\text{pit})$  than the unpitted samples during the forward scan. Although the phenomenon is easy to observe, few authors have treated this aspect of Al corrosion [24-26]. Sometimes, the potential where the steep fall of current during the reverse scan is substituted by a less potential dependent current region is called pit transition potential [27,28]. The elevated current density can be attributed to an acidified surface film which remains in the pits formed at  $E > E(\text{pit})$ . From the potential switch experiments in the present work, which showed that growing pits stop within tenths of seconds, one has to conclude that these currents are not caused by some kind of pitting corrosion which continues below  $E(\text{pit})$ , although Moore [26] tried to apply a model from Newman [29] who postulated that pits could reduce its active surface, transforming itself into tunnels below  $E(\text{pit})$ .

Morphological studies from Moore [26] showed the formation of some tunnels as postulated by the model. However, it is widely accepted that the formation of metastable pits or tunnels below  $E(\text{pit})$  occurs also at passive surfaces without previous pitting attack [25] and at the pitted surface with an acidified surface film the number of metastable pits or tunnels might be enhanced.

It is important to know that residual currents continue for several hours or even days when the reverse scan is stopped and the samples are held potentiostatically at  $E < E(\text{pit})$  [30]. The time the current needs to cease depends on the charge which had passed at  $E > E(\text{pit})$ . This shows that a quasi-stationary state exists in which the acidified electrolyte in the repassivated pits and tunnels below  $E(\text{pit})$  is maintained by diffusion and migration between the pitted surface and the neutral bulk electrolyte, thus maintaining acid attack of the surface for a long time. After the decay of the current what is found on the surface is a rounded shallow attack, instead of crystallographic pitting. The decay of current occurs because the acid attack leads to a smoothening of the surface. As a consequence the surface pH maintained by metal dissolution and transport begins to rise and the attack comes to a standstill. The attack can be considered as a kind of crevice corrosion, where the corrosion is consuming the crevice.

The decisive difference between pitting corrosion and the corrosion by residual currents below  $E(\text{pit})$  is the state of the surface. Pitting means that the surface is maintained active by some chloride containing film. Dissolution is localized and rapidly dissolving surfaces are coexisting side by side with passive surfaces. Constant attack of this kind leads to more and more roughened surfaces. Corrosion by residual currents, on the other hand, means metal dissolution through a passive film thinned by an acid electrolyte. Dissolution occurs on the whole surface, since it is determined by local pH. This leads finally to a smoothening of the surface previously roughened by pitting. The rounded, shallow attack has the morphology which is typical for Al dissolution in an acid electrolyte.

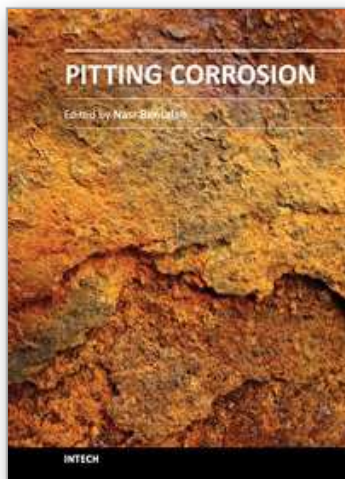
## 5. References

- [1] Beck T.R., Salt Film Formation during Corrosion of Aluminum, *Electrochimica Acta*, 29 (1984) 485-491.
- [2] Beck T.R., Mueller J.H., Conductivity and Water Permeability of Barrier-Layer  $\text{AlCl}_3$  as a Function of Temperature, *Electrochimica Acta*, 33 (1988) 1327-1333.
- [3] Beck T.R., Chan S.G., Corrosion of Magnesium at High Anodic Potentials J, *Electrochem.Soc.* 130 (1983) 1289-1295.
- [4] Streblov H.H., Ives M.B., On the electrochemical conditions within small pits, *Corr.Sci.* 16 (1976) 317-318.
- [5] Hunkeler F., Böhni H., Determination of Pit Growth-Rates on Aluminum Using a Metal Foil Technique, *Corrosion*, 37 (1981) 645-650.
- [6] Cheung W.K., Francis P.E., Turnbull A., Test Method for Measurement of Pit Propagation Rates, *Materials Science Forum* 192-194 Part1 (1995) 185-196.
- [7] Wenzel G; Knörnschild G., Kaesche H, Intergranular Corrosion And Stress-Corrosion Cracking of an Aged Alcu Alloy in 1-N Nacl Solution *Werkstoffe und Korrosion-Materials and Corrosion* 42 (1991) 449-454.
- [8] .Glenn A.M, Muster T.H., Luo C., Zhou X., Thompson G.E., Boag A., Hughes A.E., Corrosion of AA2024-T3 Part III: Propagation, *Corrosion Science* 53 (2011) 40-50.
- [9] Edeleanu C., The Propagation of Corrosion Pits in Metals, *J. Inst. Metals* 89 (1960) 90-94.
- [10] Baumgärtner M., Kaesche H., Microtunnelling During Localized Attack of Passive Aluminum - the Case of Salt Films vs Oxide-Films *Corr. Sci.* 29 (1989) 363-378.
- [11] Baumgärtner M., Kaesche H., Aluminum Pitting in Chloride Solutions - Morphology and Pit Growth-Kinetics *Corr. Sci.* 31 (1990) 231-236.
- [12] Baumgärtner M., Kaesche H., The Pitting Potential of Aluminum in Halide Solutions; *Werkstoffe und Korrosion* 42 (1991) 158-168.
- [13] Knörnschild G., Kaesche H., Localized corrosion of homogeneous binary Al-Zn and Al-Cu alloys. The Electrochemical Society Fall Meeting, Toronto, Oct.11-16, 1992, Vol.92-2, p. 178.
- [14] Kaesche H.: *Corrosion of Metals*, Springer, 2003, Chapter 12.
- [15] Frankel G.S., Pit growth in thin metallic films, *Mat. Sci. For.*, 247 (1997) 1-7.
- [16] Alwitt R.S., Uchi H., Beck T.R., Alkire R.C., Electrochemical Tunnel Etching of Aluminum, *J.Electrochem.Soc* 131 (1984) 13-17.
- [17] Alwitt R.S., Beck T.R., Hebert K., Proc. Int. Conf. Localized Corrosion, Orlando 1987, Ed. H.S.Isaacs, NACE, Houston, p.145.
- [18] Hebert K.R., Alkire R., Growth and Passivation of Aluminum Etch Tunnels, *J.Electrochem.Soc.*135 (1988 )2146-2157.
- [19] Lucente A.M., Scully J.R., Pitting and Alkaline Ddissolution of an Amorphous-Nanocrystalline Alloy with Solute-Lean Nanocrystals, *Corrosion Science* 49 (2007) 2351-2361.
- [20] Yoshioka H., Habazaki H., Kawashima A., Asami K., Hashimoto K., The Corrosion Behavior of Sputter-Deposited Al-Zr Alloys in 1-M HCl Solution *Corrosion Science* 33 (1992) 425-436.
- [21] Shaw B.A., Davis G.D., Fritz, T.L. Rees B.J., Moshier W.C., The Influence of Tungsten Alloying Additions on The Passivity of Aluminum, *J.Electrochem.Soc.* 138 (1991) 3288-3295.



- [22] Moshier W.C., Davis G.D., Ahearn J.S., and Hough H.F., Influence of Molybdenum on the Pitting Corrosion of Aluminum Films, *J. Electrochem. Soc.* 133 (1986) 1063-1064.
- [23] Asami K., Habazaki H., Inoue A., Hashimoto K., *New Frontiers Of Processing And Engineering In Advanced Materials* Book Series: Materials Science Forum Editors: M.Naka, T.Yamane, Volume 502 (2005) 225-230.
- [24] Yasuda M., Weinberg F., Tromans D., Pitting Corrosion of Al and Al-Cu Single-Crystals, *J. Electrochem. Soc.* 137 (1990) 3708-3715.
- [25] Pride S.T., Scully J.R., Hudson J.L., Metastable Pitting of Aluminum and Criteria for the Transition to Stable Pit Growth, *J. Electrochem. Soc.* 141 (1994) 3028-3040.
- [26] Moore K.L., Sykes J.M., Grant P.S., An Electrochemical Study of Repassivation of Aluminium Alloys with SEM Examination of the Pit Interiors Using Resin Replicas, *Corrosion Science* 50 (2008) 3233-3240.
- [27] Trueba M., Trasatti S.P., Study of Al Alloy Corrosion in Neutral NaCl by the Pitting Scan Technique, *Materials Chemistry and Physics* 121 (2010) 523-533.
- [28] Brunner J.G., May J., Höppel H.W., Göken M., Virtanen S., Localized corrosion of ultrafine-grained Al-Mg model alloys, *Electrochimica Acta* 55 (2010) 1966-1970.
- [29] Newman R.C., Local Chemistry Considerations in the Tunneling Corrosion of Aluminum, *Corrosion Science* 37 (1995) 527-533.
- [30] Füllmann T., Untersuchungen zum Lochfrass und zum Repassivierungsverhalten von Al und Al-Legierungen, Diploma Thesis, Erlangen 1993.

IntechOpen



### **Pitting Corrosion**

Edited by Prof. Nasr Bensalah

ISBN 978-953-51-0275-5

Hard cover, 178 pages

**Publisher** InTech

**Published online** 23, March, 2012

**Published in print edition** March, 2012

Taking into account that corrosion is costly and dangerous phenomenon, it becomes obvious that people engaged in the design and the maintenance of structures and equipment, should have a basic understanding of localized corrosion processes. The Editor hopes that this book will be helpful for researchers in conducting investigations in the field of localized corrosion, as well as for engineers encountering pitting and crevice corrosion, by providing some basic information concerning the causes, prevention, and control of pitting corrosion.

#### **How to reference**

In order to correctly reference this scholarly work, feel free to copy and paste the following:

G. Knörnschild (2012). Mechanism of Pit Growth in Homogeneous Aluminum Alloys, Pitting Corrosion, Prof. Nasr Bensalah (Ed.), ISBN: 978-953-51-0275-5, InTech, Available from:

<http://www.intechopen.com/books/pitting-corrosion/mechanism-of-pit-growth-in-aluminum-and-in-homogeneous-aluminum-alloys>

**INTECH**  
open science | open minds

#### **InTech Europe**

University Campus STeP Ri  
Slavka Krautzeka 83/A  
51000 Rijeka, Croatia  
Phone: +385 (51) 770 447  
Fax: +385 (51) 686 166  
[www.intechopen.com](http://www.intechopen.com)

#### **InTech China**

Unit 405, Office Block, Hotel Equatorial Shanghai  
No.65, Yan An Road (West), Shanghai, 200040, China  
中国上海市延安西路65号上海国际贵都大饭店办公楼405单元  
Phone: +86-21-62489820  
Fax: +86-21-62489821

© 2012 The Author(s). Licensee IntechOpen. This is an open access article distributed under the terms of the [Creative Commons Attribution 3.0 License](#), which permits unrestricted use, distribution, and reproduction in any medium, provided the original work is properly cited.

IntechOpen

IntechOpen